

Tumor-Homing Chitosan-Based Nanoparticles for Cancer Theragnosis; Imaging, Drug Delivery and Therapy

Ick Chan Kwon^{1,2,*}, Kwangmeyung Kim^{1,2}, Kyeongsoon Park^{1,2}, Seulki Lee^{1,2}, Kuiwon Choi¹, In-San Kim²

¹*Biomedical Research Center, Korea Institute of Science and Technology, 39-1 Hawolgok-dong, Seongbuk-gu, Seoul 136-791, Korea,*

²*Kist regional Laboratory in Advanced Medical Technology Cluster for Diagnosis & Prediction, Kyungpook National University, Korea*

*E-mail: ikwon@kist.re.kr

ABSTRACT

We have prepared self-assembled polymeric drug carriers containing fluorophore and loaded drugs for theragnostic imaging of tumors. This new type of polymeric drug carriers visualizes the accumulation of carriers at tumor sites, and evaluates therapeutic efficacies, and thereby providing an exciting new tool for monitoring tumor diagnosis and therapy.

1. INTRODUCTION

Theragnosis is a new concept in next-generation medicine that combines simultaneous diagnostics and therapeutics. By integration of molecular imaging and nanomedicine with chemistry, drug delivery, cell biology, and as well as clinical medicine, we developed cancer theragnosis platform technologies which enable i) specified delivery of anticancer drugs , ii) targeted visualization of cancer and iii) clinical management of cancer for early diagnostic and response to drug treatment assessment. Nano-sized tumor-homing chitosan-based nanoparticles (CNP) bearing various anticancer drugs (Paclitaxel; Docetaxel, doxorubicin, photosensitizer, etc.) and near-infrared (NIR) dye were developed and have been explored for potential applications in cancer theragnosis. With the help of state-of-the-art optical fluorescent imaging technology, targeting drug efficacy, biodistribution and optimal treatment conditions of CNPs in tumor-bearing mice can be elucidated, tracked, and monitored non-invasively in real-time. The biocompatible and biodegradable CNPs that contain encapsulated anticancer drugs accumulated selectively and efficiently in tumor and enhanced the drug efficacy with reduced toxicity. All the procedures were visualized, imaged, and analyzed in a rapid and efficient fashion by using fluorescence tomographic imaging in vivo. Its improved practical potency highlights its potential as new strategies for cancer diagnostics and targeted therapy.

2. MATERIALS AND METHODS

2.1. Tissue distribution and tumor accumulation of nanoparticles by non-invasive optical imaging system

Hydrophobically modified glycol chitosans (HGC) were prepared by coupling of glycol chitosans and 5 β -cholanic acid in the presence of EDAC. To visualize the accumulation at tumors, cyanine 5.5, a near-infrared fluorophore, was conjugated to amine group of HGC to prepared HGC-Cy5.5 probe. When tumor sizes were ranged in 50-70mm³, HGC-Cy5.5 probe

was i.v. injected via the lateral tail vein, and monitor the biodistribution and tumor accumulation of HGC-Cy5.5 and tumor accumulation. Furthermore, the therapeutic processes were evaluated by monitoring tumor sizes after i.v. injection of PTX-loaded HGC-Cy5.5. The visualization of tumor accumulation and biodistribution of polymeric drug carriers were analyzed by using Kodak Image station and GE optix explore.

3. RESULTS AND DISCUSSION

We have developed hydrophobically modified glycol chitosans (HGC) that form nano-sized particles in aqueous media. The mean diameters of the three glycol chitosan nanoparticles did not vary greatly, ranging from 231 to 310 nm, and all showed a good colloidal stability in PBS at 37°C (data not shown), as well as similar surface charge.

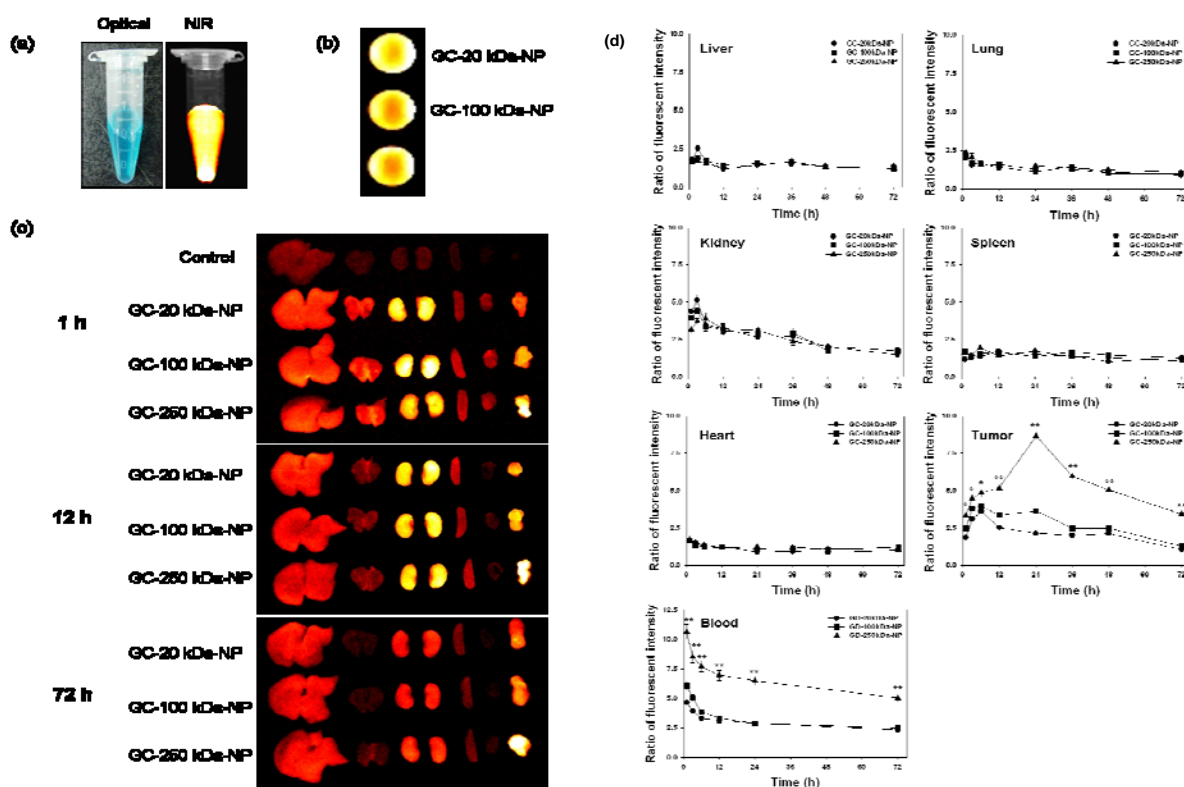


Fig. 1. Near-infrared (NIR) fluorescence images of Cy5.5-labeled glycol chitosan nanoparticles and ex vivo NIRF images of dissected organs and tumors. (a) White light and NIR fluorescence images of Cy5.5-labeled glycol chitosan nanoparticles. (b) Near-infrared fluorescence intensities of GC-20 kDa-NP, GC-100 kDa-NP, and GC-250 kDa-NP are similar. (c) Representative ex vivo NIR fluorescence images of dissected organs of mice bearing SCC7 tumors. 1: liver; 2: lung; 3: kidney; 4: spleen; 5: heart; and 6: tumor. (d) Quantitative results of tissue distribution and tumor accumulation for three glycol chitosan nanoparticles.

In *ex vivo* NIR images at 1 h post-injection, strong fluorescence intensities for GC-20 kDa-NP and GC-100 kDa-NP were observed in the kidney, indicating rapid excretion of these nanoparticles from the body (Fig. 1c). On the other hand, GC-250 kDa-NP displayed stronger fluorescence intensity in the tumor, relative to the organs. After 12 h post-injection, NIR

fluorescence intensity in the tumor and kidney was increased, whereas that in other organs, such as liver, lung, spleen and heart, was gradually decreased. After 3 days post-injection, NIR fluorescence intensity was significantly decreased in all tissues, except tumor. Moreover, fluorescence intensities of the nanoparticles in tumors increased with molecular weight. Our data imply that tumor accumulation of glycol chitosan nanoparticles is dependent on the molecular weight. Fig. 1d displays the detailed quantitative results on tissue distribution and tumor accumulation. The uptake of particles in the spleen was not significant, compared to other tissues. Glycol chitosan nanoparticles may not stimulate macrophages in the spleen, and thus not subjected to opsonization or removal by the reticuloendothelial system (RES). The distribution of glycol chitosan nanoparticles in the kidney varies according to molecular weight within 3 h post-injection. GC-20kDa-NP and GC-100kDa-NP uptake in the kidney was higher (up to 1.4- and 1.2-fold, respectively) than that of GC-250kDa-NP ($p < 0.05$). However, after 6 h post-injection, the three glycol chitosan nanoparticles in the kidney displayed similar distribution patterns. It is likely that GC-20kDa-NP and GC-100kDa-NP are rapidly excreted from the body within a relatively short time, compared to GC-250 kDa-NP. The tumor targeting characteristics of glycol chitosan nanoparticles were significantly dependent on molecular weight. The NIR fluorescence intensities of GC-20kDa-NP and GC-100kDa-NP in the tumor increased slightly at 6 h post-injection, and decreased gradually thereafter. However, GC-250 kDa-NP displayed strong fluorescence intensity at 1 day, which was maintained up to 3 days. At 24 h post-injection, the NIR fluorescence intensity of GC-250kDa-NP was higher than those of GC-20kDa-NP and GC-100kDa-NP (up to 4.1- and 2.4-fold, respectively). The high tumor targeting efficiency of GC-250 kDa-NP is supported by data on blood circulation time. GC-250 kDa-NP was detected at elevated levels in the blood for 3 days, implying stability in the bloodstream and maintenance of an intact nanostructure. In contrast, the other glycol chitosan nanoparticles with lower tumor selectivity were maintained at a low level, which rapidly decreased in the bloodstream. These results indicate that while all three glycol chitosan nanoparticles accumulate at the tumor sites, their tumor distribution is distinct, depending on the molecular weight.

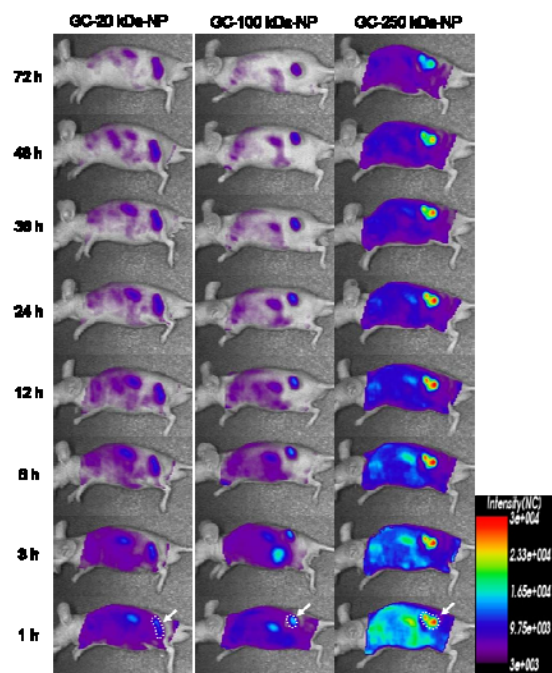


Fig. 2. In vivo non-invasive NIR fluorescence images of real-time tumor targeting characteristics of glycol chitosan nanoparticles. The tumor location is specified with an arrow. (left figure)

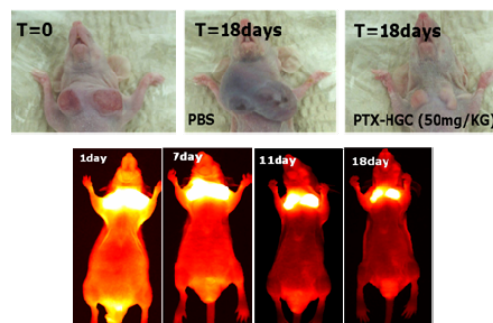


Fig. 3. Monitoring the body distribution and therapeutic responses by PTX-loaded HGC-Cy5.5 nanoparticles in mice bearing B16F10 melanoma.

The time-dependent excretion profile and tumor accumulation of glycol chitosan nanoparticles in SCC7 tumor-bearing athymic nude mice were evaluated using the eXplore Optix system (Fig. 2). The excretion profile of glycol chitosan nanoparticles in live animals was clearly visualized by monitoring real-time NIR fluorescence intensity in the whole body. Consistent with tissue distribution and blood circulation profiles (Fig.1), the NIR fluorescence intensities of GC-20kDa-NP and GC-100kDa-NP rapidly decreased in the whole body within 6 h post-injection, possibly due to clearance through urinary excretion. However, the high fluorescence intensity of GC-250kDa-NP was maintained in the whole body up to 3 days, implying prolonged circulation time and effective tumor accumulation.

From these above results, HGC-Cy5.5 probe accumulated into tumors was gradually excreted from tumors. At 72h, most of HGC-Cy5.5 was washed out at tumors even though it is still remained. Thus, we decided that the frequency of injection time for HGC-Cy5.5 is once every 4 day. HGC-Cy5.5 containing paclitaxel (PTX) could simply evaluate the therapeutic processes of B16F10 tumor by visualizing its accumulation and tumor sizes as shown in Fig. 4. Injection of PTX-HGC nanoparticles into the tail vein of tumor-bearing mice efficiently prevented the tumor growth (Fig. 3), and less toxic to the tumor-bearing mice and increased survival time when formulated in HGC nanoparticles than when formulated with Cremophor EL. HGC nanoparticles have excellent potential as a carrier of PTX and other cancer drugs.

4. CONCLUSIONS

Fluorescent labeled drug carriers can monitor the accumulation at tumors, biodistribution, and the frequency of drug injection and therapeutic processes. Therefore, combination of tumor targeting therapy, and imaging in an all-in-one system provides a useful multi-modal approach in the battle against cancer and displays a new field in which this new technology has set the stage for an evolutionary leap in therapy and diagnosis of human cancer.

5. REFERENCES

- [1] J.H. Park, Y.W. Cho, H. Chung, I.C. Kwon, S.Y. Jeong. *Biomacromolecules* 4 (2003) 1087.
- [2] S. Kwon, J.H. Park, H. Chung, I.C. Kwon, S.Y. Jeong, I.S. Kim. *Langmuir* 19 (2003) 10188.
- [3] J.H. Park, S. Kwon, J.O. Nam, R.W. Park, H. Chung, S.B. Seo, I.S. Kim, I.C. Kwon, S.Y. Jeong. *J. Control. Release* 95 (2004) 579.
- [4] K. Kim, J.H. Kim, S. Kim, H. Chung, K. Choi, I.C. Kwon, J.H. Park, Y.S. Kim, R.W. Park, I.S. Kim, S.Y. Jeong. *Macromol. Res.* 13 (2005) 167.
- [5] J.H. Kim, Y.S. Kim, J.H. Park, K. Kim, K. Choi, H. Chung, S.Y. Jeong, R.W. Park, I.S. Kim, I.C. Kwon. *J. Control. Release* 111 (2006) 228.
- [6] K. Park, J.H. Kim, Y.S. Nam, S. Lee, H.Y. Nam, K. Kim, J.H. Park, I.S. Kim, K. Choi, S.Y. Kim, I.C. Kwon. *J. Control. Release* 2007, doi:10.1016/j.jconrel.2007.04009.